



Contents lists available at ScienceDirect

Journal of Materiomics

journal homepage: [www.journals.elsevier.com/journal-of-materiomics/](http://www.journals.elsevier.com/journal-of-materiomics/)

Research paper

# Genetic algorithm-enabled mechanical metamaterials for vibration isolation with different payloads



Xinyu Song<sup>a</sup>, Sen Yan<sup>b</sup>, Yong Wang<sup>c</sup>, Haojie Zhang<sup>a</sup>, Jiacheng Xue<sup>a</sup>, Tengfei Liu<sup>a</sup>, Xiaoyong Tian<sup>a</sup>, Lingling Wu<sup>a,\*</sup>, Hanqing Jiang<sup>d,e,f,\*\*</sup>, Dichen Li<sup>a</sup>

<sup>a</sup> State Key Laboratories for Manufacturing Systems Engineering, Xi'an Jiaotong University, Xi'an, 710049, China

<sup>b</sup> Metamaterials Laboratory, School of Materials Science and Engineering, Tsinghua University, Beijing, 100084, China

<sup>c</sup> School of Aeronautics and Astronautics, Zhejiang University, Hangzhou, 310027, China

<sup>d</sup> School of Engineering, Westlake University, Hangzhou, 310030, China

<sup>e</sup> Westlake Institute for Advanced Study, Hangzhou, 310024, China

<sup>f</sup> Research Center for Industries of the Future, Westlake University, Hangzhou, 310030, China

## ARTICLE INFO

### Article history:

Received 10 September 2024

Accepted 17 September 2024

Available online 15 October 2024

### Keywords:

Mechanical metamaterials

Machine learning

Multi-payload

Quasi-zero stiffness

Vibration isolation

## ABSTRACT

Mechanical vibration isolation with adaptable payloads has always been one of the most challenging topics in mechanical engineering. In this study, we address this problem by introducing machine learning method to search for quasi-zero stiffness metamaterials with arbitrarily predetermined payloads and by employing multi-material 3D printing technology to fabricate them as an integrated part. Dynamic tests demonstrate that both the single- and multi-payload metamaterials can effectively isolate mechanical vibration in low frequency domain. Importantly, the payload of the metamaterial could be arbitrarily designed according to the application scenario and could function at multiple payloads. This design strategy opens new avenues for mechanical energy shielding under various scenarios and under variable loading conditions.

© 2024 The Authors. Published by Elsevier B.V. on behalf of The Chinese Ceramic Society. This is an open access article under the CC BY-NC-ND license (<http://creativecommons.org/licenses/by-nc-nd/4.0/>).

## 1. Introduction

Metamaterials[1–3] have provided an effective route to solve the crucial problems in industry, examples include electromagnetic (EM) cloak [4,5], perfect lens [6], EM absorber [7], and so on [8,9]. In the field of mechanical metamaterials, extraordinary properties, such as negative Poisson's ratio [10,11], negative thermal expansion [12,13], multistability [14,15], and elastomechanical cloaking [16], have been proposed to achieve versatile functionalities, including impact energy dissipation/absorption, acoustic wave manipulation [17,18], mechanical vibration shielding and so on. Among them, full frequency band vibration isolation with adaptable payloads has always been one of the most difficult problems to be solved. Because most of the time, mechanical vibrations in low and

ultralow frequency (e.g., lower than 10 Hz) are harmful to our health [19,20]. Besides, vibrations will bring measurement errors and shorten the working life of precision instruments.

Recent advances in machine learning [21], and three-dimensional (3D) printing [22] are transforming our design from imagination into realistic artificial structures. On this basis, various mechanical metamaterials with high-static-low-dynamic-stiffness performance for low-frequency vibration isolation performance have been proposed[23–25]. Most of them are designed based on the quasi-zero stiffness mechanism by combining negative and positive modules appropriately to create an effective stiffness close to zero in specific displacement region [26–28]. This method is highly effective to solve the inherent contradictory between low-frequency vibration isolation performance and payload capacity in traditional vibration isolation materials (foams, springs, etc.). However, there are also some aspects to be improved. Firstly, on the aspect of designing methodology, most of the proposed works are achieved based on *ad hoc* method, a trial-and-error process that is highly dependent on the intelligence of researchers and could be inefficient and time-wasting [29]. Secondly, the vibration isolation performance of achieved metamaterials in low/ultra-low frequency

\* Corresponding author.

\*\* Corresponding author. School of Engineering, Westlake University, Hangzhou, 310030, China.

E-mail addresses: [lingling.wu@xjtu.edu.cn](mailto:lingling.wu@xjtu.edu.cn) (L. Wu), [hanqing.jiang@westlake.edu.cn](mailto:hanqing.jiang@westlake.edu.cn) (H. Jiang).

Peer review under responsibility of The Chinese Ceramic Society.

band is often unsatisfactory as a result of the inefficiency of design method. It is still difficult to achieve low frequency vibration isolation and the designed working range of displacement is usually too narrow that could not fulfill the practical application under large vibration amplitude [30]. Thirdly, most of the reported metamaterials are usually designed for one single payload or multiple payloads by simply connecting unit cells in series[31–33], and arbitrarily pre-determined multi-payload is still under investigation. Lastly, in terms of fabrication, mechanical metamaterials with excellent vibration isolation performance are often fabricated by traditional assembly method, which is inconvenient, high-cost, and will bring assembly error in the structure [34,35]. Recently reported works have employed 3D printing to fabricate their metamaterials as an integrated part. Most of them are printed with only one material (either rigid or soft) [32], which limits the design space and usually lead to great difference of geometric size of different areas in the metamaterial.

Here, to address the above-mentioned challenges, we introduce a machine learning-based modular design method to search for the optimal quasi-zero stiffness metamaterials with arbitrarily pre-determined single- or multi-payloads. The metamaterials are fabricated by multi-material 3D printing technology which could deposit rigid and soft materials simultaneously in one integrated sample. Dynamic experiments demonstrate the vibration isolation performance of the proposed metamaterials with different payloads. These metamaterials offer a novel design approach in multi-payload mechanical metamaterials for vibration isolation applications.

## 2. Experimental section

### 2.1. Machine learning design process

The design of the quasi-zero stiffness meta-atom starts with a typical quasi-zero stiffness design as presented in Fig. 1a [26]. The model combines negative element (side tilting beams) with positive element (curved beams in the middle). To identify the optimal combinations of geometric parameters for the quasi-zero stiffness meta-atom that would satisfy the desired working payload, a genetic algorithm (GA) combined with Finite element analysis (FEA) was applied. The structural evolution process was performed to find out the optimal meta-atom. GA could be readily combined with the COMSOL Multiphysics finite element simulations via LiveLink™ for MATLAB®. Details could be found in the literature [36]. By applying GA, a population size of 30 quasi-zero stiffness meta-atoms is initially generated. Static analysis will be performed to calculate the force-displacement curve of each meta-atom, from which we take a series of points and compare their force value with our desired payload value (Fig. 1b), and calculate the error to evaluate the fitness function.

Then, the genetic algorithm is employed to find out an optimal solution by genetically breeding a population of individuals over a series of generations until the change of fitness function between two adjacent generations is smaller than the tolerance.

Based on the fitness value, we sort and perform roulette wheel selection operations on the population, choosing individuals with higher fitness to proceed to the next generation. Then, we apply crossover and mutation operations to generate new individuals (Fig. 1c). The crossover operation generates new offspring individuals by combining parts of the features of two parent individuals. The mutation operation introduces new variations by randomly changing some features of an individual.

### 2.2. Fabrication of the metamaterials

The metamaterial samples are then fabricated using the multi-material fused deposition modeling (FDM) technology (BlueMaker 335, BlueMaker Technology Group, Shenzhen, China). The schematic of multi-material FDM process is presented by Fig. 1d. In our research work, we adopt PLA as rigid material (PLA Matte, Bambu Lab, Density  $\rho_{\text{rigid}} = 1310 \text{ kg/m}^3$ , Young's modulus  $E_{\text{rigid}} = 2360 \text{ MPa}$ ) and TPU as soft material (TPU 95A HF, Bambu Lab, Density  $\rho_{\text{soft}} = 1220 \text{ kg/m}^3$ , Young's modulus  $E_{\text{soft}} = 29 \text{ MPa}$ ).

## 3. Results and discussion

### 3.1. Finite element analysis simulation

We start the design of a single payload mechanical metamaterial by employing the above-mentioned machine learning method. The initial structure of the meta-atom we choose in this work is a typical quasi-zero stiffness structure that combine negative element (side tilting beams) with positive element (curved beams in the middle), which is characterized by 8 parameters, including  $a$ ,  $c$ ,  $d$ ,  $h$ ,  $r$ ,  $l$ ,  $\theta$  as presented in Fig. 2a, and the out-of-plane thickness of the model  $b$ .

Because of the calculation cost during the GA evolution, we choose an acceptable mesh size to ensure the design accuracy and FEM calculation cost. In the future study, we will choose smaller mesh size and more accurate material parameters to improve the FEM calculation accuracy. Here, to validate the designing process, we set a payload goal as 3 N. By employing genetic algorithm combined with finite element analysis, we obtained an iteration process described by Fig. 2b, from which we can see that the result converged at about 70th generation. To validate the searching result, we plot the force-displacement curves of the best meta-atom individuals in the 1st generation, 6th generation, and 70th generation, respectively, as presented in Fig. 2c. We could see that the best meta-atom in 70th generation shows quasi-zero stiffness corresponding to our target payload of 3 N, while those meta-atoms in 1st and 6th generation present great discrepancy. We also provide the simulated deformation images of the optimal meta-atom in Fig. 2d, which demonstrates a working displacement range from 4 mm to 16 mm with quasi-zero stiffness property.

Based on the successful searching of meta-atom with one single payload, we then developed the mechanical metamaterial with multi-payload by using the same machine learning method. The schematic illustration of the metamaterial with two staged payloads is presented in Fig. 3a, which is characterized by 15 parameters, including  $a_1$ ,  $a_2$ ,  $h_1$ ,  $h_2$ ,  $h_3$ ,  $h_4$ ,  $r_1$ ,  $r_2$ ,  $c_1$ ,  $c_2$ ,  $d_1$ ,  $d_2$ ,  $\theta_1$ ,  $\theta_2$ , and the out-of-plane thickness of the model  $b$ .

The two payload stages we set as the optimization goal in this work is arbitrarily selected as  $F_1 = 3 \text{ N}$ , and  $F_2 = 7 \text{ N}$ . The iteration process is presented in Fig. 3b, from which we could see that an optimal result that could fulfil our requirement is achieved in 60th generation. Just like the meta-atom with single payload, we plot the force-displacement curves of the best meta-atom individuals in the 1st generation, 10th generation, and 60th generation, respectively, as presented in Fig. 3c, to compare the static mechanical performance of them. We could see that the best meta-atom in 60th generation shows a clear 2-staged quasi-zero stiffness plateau corresponding to our target payload of  $F_1 = 3 \text{ N}$  and  $F_2 = 7 \text{ N}$ , respectively. By contrast, the meta-atoms in 1st and 10th generation shows more or less some deviations from our designing goals. The simulated deformation images of the optimal meta-atom in 60th generation are presented in Fig. 3e, corresponding to the initial configuration ①, configuration ② with displacement of 5 mm and ③ with displacement of 10 mm, respectively, which

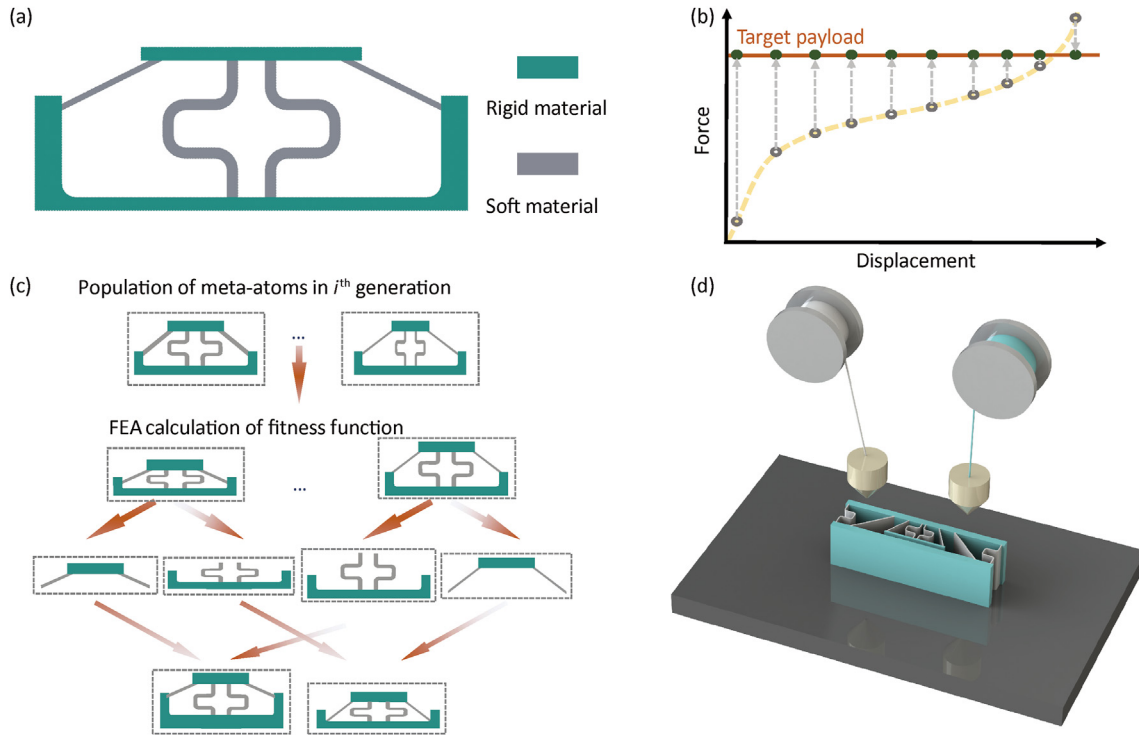


**Fig. 1.** Concept of investigation process of quasi-zero stiffness mechanical metamaterial for vibration isolation. (a) A zero stiffness meta-atom by combining positive and negative modules. The green and gray material represent rigid and soft material, respectively. (b) Several points on the force-displacement curves are employed to compare with the desired payloads and evaluate the quasi-zero stiffness performance of the meta-atom. (c) Schematic illustration for the genetic algorithm employed to search for the optimal quasi-zero stiffness meta-atom. (d) Schematic of multi-material 3D printing technology to fabricate the quasi-zero stiffness meta-atom.

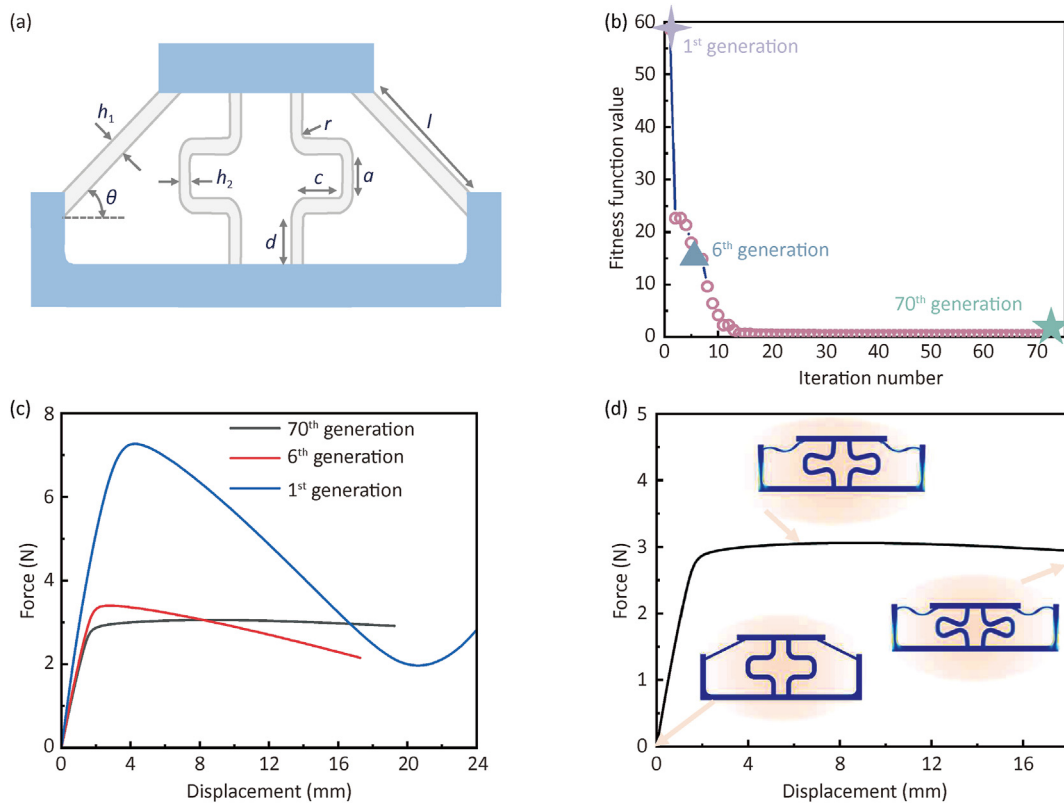


**Fig. 2.** Design of the mechanical metamaterial with single payload by machine learning method. (a) Schematic illustration of the quasi-zero stiffness meta-atom with single payload. (b) Iteration history of the meta-atom. (c) Force-displacement curves of the best meta-atom individuals in the 1<sup>st</sup> generation, 6<sup>th</sup> generation, and 70<sup>th</sup> generation, respectively (d) Simulated deformation process and mechanical behavior of the optimal meta-atom.

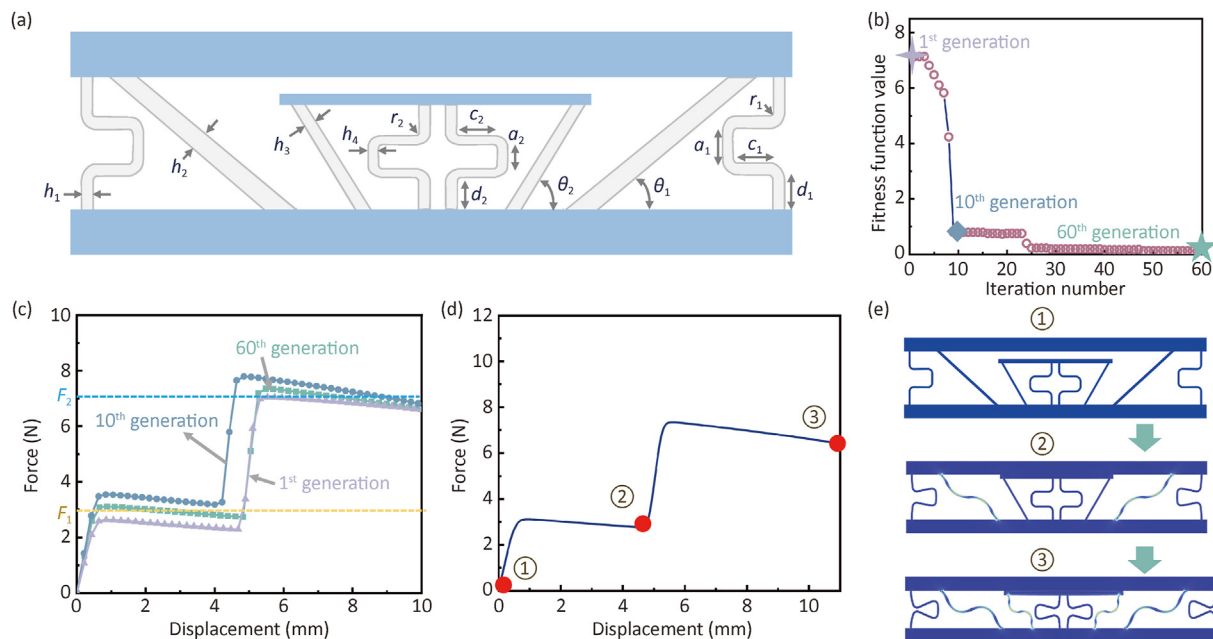


**Fig. 3.** Design of the mechanical metamaterial with two predetermined payloads by machine learning method. (a) Schematic illustration of the two-stage payload quasi-zero stiffness meta-atom. (b) Iteration history of the two-stage payload meta-atom. (c) Force-displacement curves of the best two-stage payload meta-atom individuals in the 1st generation, 10th generation, and 60th generation, respectively (d) The force displacement curve of the optimal structure. (e) Simulated deformation process of the optimal two-stage payload meta-atom.

shows that the working range of the first stage payload is approximately from 1 mm to 5 mm, and the working range of the second stage payload is from 6 mm to 10 mm. From Fig. 3e we could also conclude that, under payload of 3 N, the first stage vibration isolation (displacement from 1 mm to 5 mm) is only supported by the tilting/curved beam components that distributed on the side of the meta-atom. When a payload of 7 N is applied, the metamaterial will deform in the range of 6 mm to 10 mm, and both the tilting/curved beam components in the middle and side will be activated, which supply a higher payload capacity.

### 3.2. Static and dynamic experiments

By using multi-material 3D printing technology, we fabricated metamaterials with both single and multi-payload vibration isolation performance. To ensure the stability of the sample and facilitate the dynamic experiment process, the single payload unit cell is fabricated with a larger thickness, while keeping other parameters the same, which result in a working payload of 9 N. To ensure the stability of the sample during dynamic experiment, we fabricate a 3-unit cells metamaterial, as presented by Fig. 4a, which has a theoretical working payload of 27 N.

For the multi-payload metamaterial, we fabricated 2 types of samples, a metamaterial with array of 4 units, and an orthogonal sample with two pieces of units with higher thickness. The 4-unit array sample has a theoretical two-stage working payload of 12 N and 28 N, while the orthogonal sample has a theoretical two-stage working payload of 30 N and 70 N. The photographs of the samples are presented in Fig. 4a–b. Displacement-controlled loading tests are conducted on the 3D printed metamaterial samples, as shown in Fig. 4c. The force-displacement curves demonstrate the quasi-zero stiffness of the mechanical metamaterials with both single and multi-payload designs. The discrepancies from the measurement result and our design target are mainly attributed to the viscous effect of TPU material, the 3D printing fabrication error (warping of the attaching surface with the platform, anisotropy

along different printing directions, etc.) and also the measurement inaccuracy. In our simulation, to save calculation time, we didn't consider the viscous effect of the TPU material. In our future work, we will add this effect in our simulation to improve the calculation accuracy.

According to the static measurement result, we determined the actual working payload for both the single and multi-payload mechanical metamaterials, which guided us to perform the dynamic experiments. Vibration tests are carried out in low-frequency ranges (1–50 Hz) to verify the vibration isolation performance. The transmission loss in dB is adopted to evaluate vibration isolation performance under different payloads. The transmission loss is defined as  $20\lg(a_{\text{output}}/a_{\text{input}})$ , where  $a_{\text{input}}$  is the amplitude of acceleration at the top of the metamaterial isolator and  $a_{\text{output}}$  is the amplitude of acceleration produced by the shaker. The measurement results are presented in Fig. 5. From the dynamic performance of the single payload metamaterial under three different payloads (Fig. 5a) we could find that, it could provide vibration isolation starting from 8 Hz. Fig. 5b presents the time domain result of the single payload metamaterials under payload of 2950 g. From the result we could see that the metamaterials show great mechanical vibration isolation performance under a frequency sweep input. During the dynamic test, continuous vibration excitation was applied to the bottom of the sample via the shaker, and a quick frequency sweep from 1 Hz to 50 Hz was performed. The signal data was then stored and filtered to remove noise using the computer. The discrepancies of the load value between the static and dynamic loads are mainly resulted from the viscous effect of the TPU material. In our future work, we will try to adopt materials with simultaneously high toughness and lower viscous effect to improve the consistency between dynamic load and static load.

For the multi-payload metamaterial composed by 4-unit cells, we could find that its first stage performance (Fig. 5b) shows vibration isolation performance starting from about 10.5 Hz for its first level payload, and an isolation frequency starting from 12.5 Hz

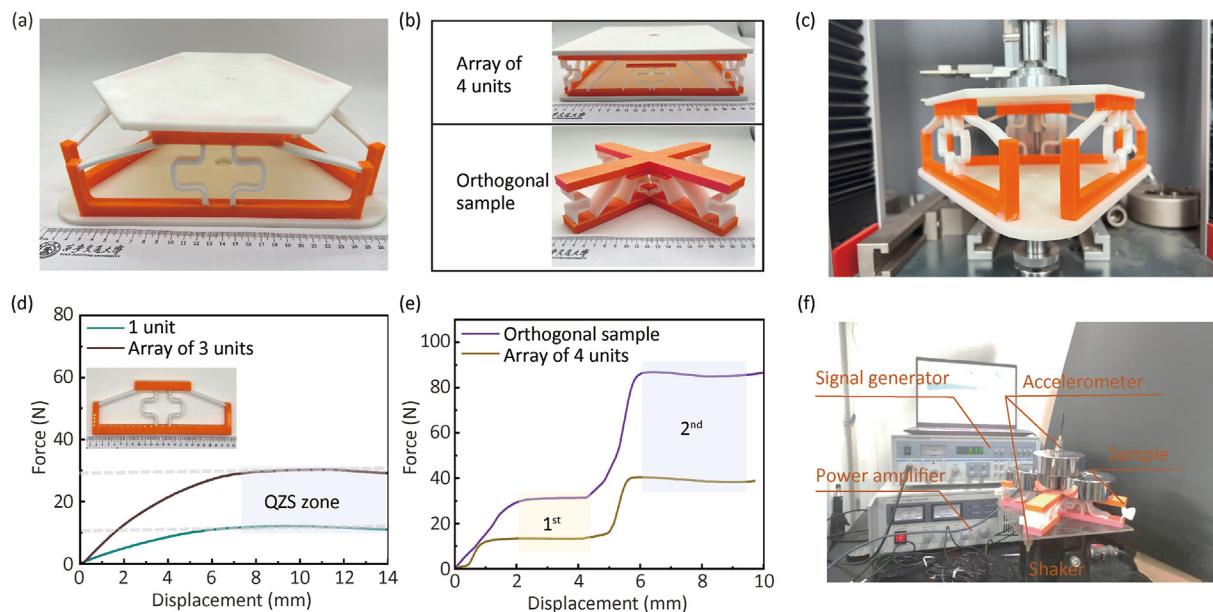


**Fig. 4.** 3D printed metamaterial samples and measurement setup. (a) Photograph of the 3D printed single payload metamaterial sample. (b) Photograph of the 3D printed multi-payload mechanical metamaterial samples. (c) Static experiment setup. Force–displacement curve of metamaterials with (d) single payload performance and (e) multi-payload performance. (f) Dynamic experiment setup.

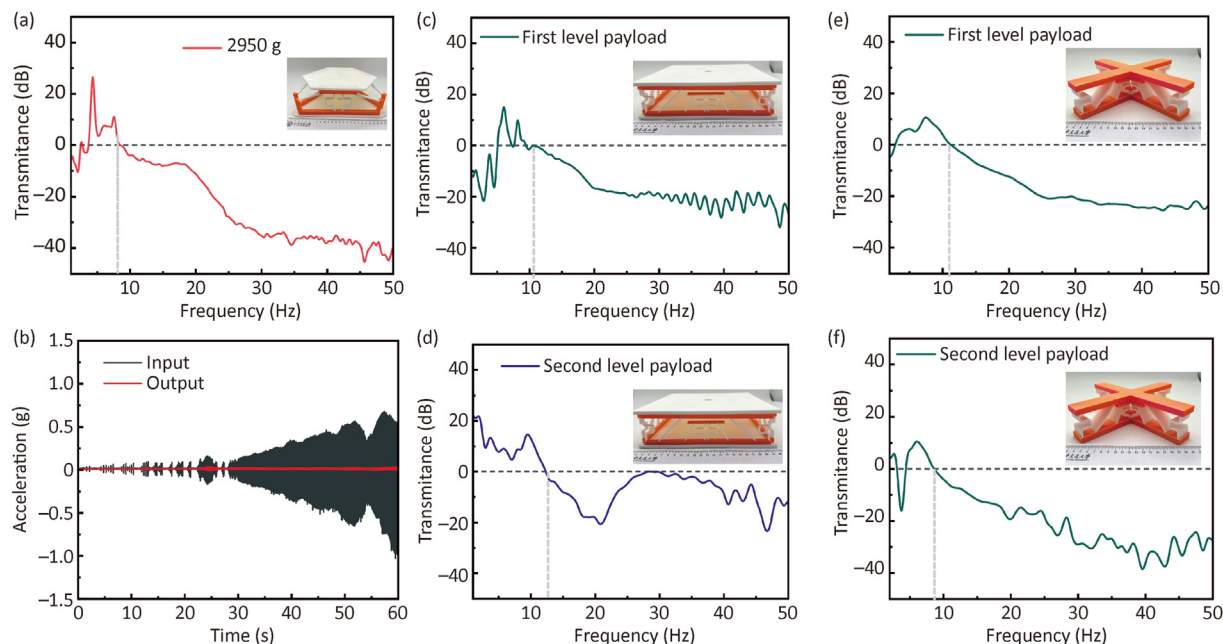


**Fig. 5.** Dynamic test of mechanical metamaterials with single and multi-payload vibration isolation performance. (a) Transmission loss of the single stage mechanical metamaterial under a payload of 2950 g. (b) The output and input acceleration amplitude for single stage mechanical metamaterial with payload of 2950 g. (c) The transmission loss of the 4-unit multi-payload mechanical metamaterial under its first stage working payload. (d) Transmission loss of the 4-unit multi-payload mechanical metamaterial under its second stage working payload. (e) Transmission loss of the orthogonal multi-payload mechanical metamaterial under its first stage working payload. (f) Transmission loss of the orthogonal multi-payload mechanical metamaterial under its second stage working payload.

for its second working payload as shown by Fig. 5c and 5d. We also measured the dynamic performance for the orthogonal sample, which presents a first level vibration isolation frequency starting from 11 Hz and a second level vibration isolation frequency starting from 9 Hz. More detailed dynamic experiment results when the metamaterials are tested under different payloads are presented from Figs. S1–S5 in the Supporting Information. The discrepancy of working payload for stable and dynamic experiment is probably

derived from the viscoelasticity performance of the TPU material [37].

By comparing the dynamic performance of the single payload metamaterial and multi-payload metamaterials, we could conclude that the vibration isolation performance under low-frequency range of the single payload metamaterial is superior to the multi-payload sample, this is mainly derived from two factors.

Firstly, by comparing Figs. 2d and 3d, we can see that the single

payload metamaterial shows better quasi-zero stiffness performance than the multi-payload metamaterial. Because of the calculation cost, we only carried out an iteration process of 60 generation for the multi-payload metamaterial to balance the design accuracy and the efficiency, which gave us a local optimal solution. We can see a slight negative stiffness trend for the multi-payload metamaterial from Fig. 3d. In our future study, we will improve our design structure and simplify the parameters, to carry out more iteration generations with better quasi-zero stiffness performance.

Secondly, for the single payload metamaterial, the triangle array is relatively more stable. While for the multi-payload metamaterials, both the 4-unit sample and the orthogonal sample present instability during the measurement. The insect component for the second level payload might contact the top surface during vibration, which brings some interference during testment.

#### 4. Conclusions

The proposed machine learning-based method to design mechanical metamaterials in this paper offer a convenient and easy-operating route to achieve mechanical vibration isolation with arbitrarily targeting single or multi-payload. By combining GA with FEA, various mechanical metamaterials could be achieved with high efficiency. Multi-material 3D printing method also broadened the designing space of the metamaterial and could ensure an integrated fabrication of the samples. The performance of the metamaterials is validated through static and dynamic tests, demonstrating their capability to effectively isolate mechanical vibrations with adaptable payloads in relatively low frequency band with a wide displacement working range. With these characteristics and advantages, the mechanical metamaterials show great potential in protecting human beings and precision instruments under complicated working environments. Future research can explore the use of other high-performance 3D printing materials to further enhance the robustness of the metamaterial. Our proposed metamaterial represents a great candidate for mechanical metamaterials with excellent mechanical shielding in the fields of aerospace engineering, civil engineering, automobile engineering and so on.

#### CRediT authorship contribution statement

**Xinyu Song:** Conceptualization, Data curation, Formal analysis, Investigation, Methodology, Resources, Software, Validation, Visualization, Writing – original draft, Writing – review & editing, Ji Zhou, Conceptualization, Data curation, Formal analysis. **Sen Yan:** Data curation, Investigation, Methodology, Resources, Software, Validation, Visualization, Writing – original draft. **Yong Wang:** Formal analysis, Investigation, Methodology, Supervision, Validation, Visualization, Writing – original draft, Writing – review & editing. **Haojie Zhang:** Conceptualization, Data curation, Investigation, Methodology. **Jiacheng Xue:** Conceptualization, Data curation, Formal analysis. **Tengfei Liu:** Conceptualization, Data curation, Funding acquisition, Investigation. **Xiaoyong Tian:** Data curation, Funding acquisition, Investigation, Jingbo Sun, Conceptualization, Data curation, Funding acquisition, Investigation. **Lingling Wu:** Conceptualization, Data curation, Formal analysis, Funding acquisition, Investigation, Methodology, Project administration, Resources, Software, Supervision, Validation, Visualization, Writing – original draft, Writing – review & editing. **Hanqing Jiang:** Conceptualization, Data curation, Formal analysis, Funding acquisition. **Dichen Li:** Conceptualization, Data curation, Formal analysis.

#### Data availability statement

The data that support the findings of this study are available from the corresponding author upon reasonable request.

#### Declaration of interests

The authors declare that they have no known competing financial interests or personal relationships that could have appeared to influence the work reported in this paper.

#### Acknowledgements

Lingling Wu acknowledges support from the National Key Research and Development Program of China (No.2022YFB3806101), the Young Elite Scientists Sponsorship Program by CAST (No. 2023QNR001) and the Key Research and Development Program in Shaanxi Province (No. 2021LLRH-08-17).

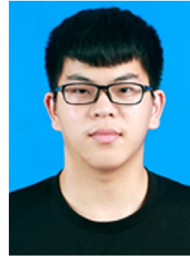
#### Appendix A. Supplementary data

Supplementary data to this article can be found online at <https://doi.org/10.1016/j.jmat.2024.100944>.

#### References

- [1] Pendry JB, Schurig D, Smith DR. Controlling electromagnetic fields. *Science* 2006;312(5781):1780–2.
- [2] Smith DR, Pendry JB, Wiltshire MCK. Metamaterials and negative refractive index. *Science* 2004;305(5685):788–92.
- [3] Barchiesi E, Spagnuolo M, Placidi L. Mechanical metamaterials: a state of the art. *Math Mech Solid* 2018;108128651773569.
- [4] Schurig D, Mock JJ, Justice BJ, et al. Metamaterial electromagnetic cloak at microwave frequencies. *Science* 2006;314(5801):977–80.
- [5] Shin D, Urzhumov Y, Jung Y, Kang G, Baek S, Choi M, et al. Broadband electromagnetic cloaking with smart metamaterials. *Nat Commun* 2012;3:1213.
- [6] Pendry JB. Negative refraction makes a perfect lens. *Phys Rev Lett* 2000;85(18):3966–9.
- [7] Landy NI, Sajuyigbe S, Mock JJ, Smith DR, Padilla WJ. Perfect metamaterial absorber. *Phys Rev Lett* 2008;100(20):207402.
- [8] Litchinitser NM, Sun J. Optical meta-atoms: going nonlinear. *Science* 2015;350(6264):3.
- [9] Zheludev NI, Plum E. Reconfigurable nanomechanical photonic metamaterials. *Nat Nanotechnol* 2016;11(1):16–22.
- [10] Clausen A, Wang F, Jensen JS, Sigmund O, Lewis JA. Topology optimized architectures with programmable Poisson's ratio over large deformations. *Adv Mater* 2015;27(37):5523–7.
- [11] Huang C, Chen L. Negative Poisson's ratio in modern functional materials. *Adv Mater* 2016;28(37):8079–96.
- [12] Wang Q, Jackson JA, Ge Q, Hopkins JB, Spadaccini CM, Fang NX. Lightweight mechanical metamaterials with tunable negative thermal expansion. *Phys Rev Lett* 2016;117(17):175901.
- [13] Zhu H, Fan T, Peng Q, Zhang D. Giant thermal expansion in 2D and 3D cellular materials. *Adv Mater* 2018;30(18):1705048.
- [14] Rafsanjani A, Akbarzadeh A, Pasini D. Snapping mechanical metamaterials under Tension. *Adv Mater* 2015;27(39):5931–5.
- [15] Shan S, Kang SH, Raney JR, Wang P, Fang L, Candido F, et al. Multistable architected materials for trapping elastic strain energy. *Adv Mater* 2015;27(29):4296–301.
- [16] Buckmann T, Thiel M, Kadic M, Schittny R, Wegener M. An elasto-mechanical unfeelability cloak made of pentamode metamaterials. *Nat Commun* 2014;5:4130.
- [17] Zhang S, Xia C, Fang N. Broadband acoustic cloak for ultrasound waves. *Phys Rev Lett* 2011;106(2):024301.
- [18] Xu X, Barnhart MV, Li X, Chen Y, Huang G. Tailoring vibration suppression bands with hierarchical metamaterials containing local resonators. *J Sound Vib* 2019;442:237–48.
- [19] Zheng G, Qiu Y, Griffin MJ. An analytic model of the in-line and cross-axis apparent mass of the seated human body exposed to vertical vibration with and without a backrest. *J Sound Vib* 2011;330(26):6509–25.
- [20] Gailiūnienė L, Krutulytė G, Šiaučūnaitė V, Savickas R, Venslauskas M. The effect of low frequency 2-10 Hz vibrations on blood circulation in lower extremities. *J Vibroeng* 2017;19(6):4694–701.
- [21] Butler K, Davies D, Cartwright H, Isayev O, Walsh A. Machine learning for molecular and materials science. *Nature* 2018;559(7715):547–55.
- [22] Truby RL, Lewis JA. Printing soft matter in three dimensions. *Nature* 2016;540(7633):371–8.

- [23] Lu Z, Brennan M, Ding H, Chen L. High-static-low-dynamic-stiffness vibration isolation enhanced by damping nonlinearity. *Sci China Technol Sci* 2018;62(7):1103–10.
- [24] Hao R, Lu Z, Ding H, Chen L. A nonlinear vibration isolator supported on a flexible plate: analysis and experiment. *Nonlinear Dynam* 2022;108(2):941–58.
- [25] Noh J, Yoon YJ, Kim P. An hysteretic high-static–low-dynamic stiffness vibration isolators with tunable inertial nonlinearity. *Nonlinear Dynam* 2023;112(4):2569–88.
- [26] Cai C, Zhou J, Wu L, Wang K, Xu D, Ouyang H. Design and numerical validation of quasi-zero-stiffness metamaterials for very low-frequency band gaps. *Compos Struct* 2020;236:111862.
- [27] Cai C, Zhou J, Wang K, Xu D, Wen G. Metamaterial plate with compliant quasi-zero-stiffness resonators for ultra-low-frequency band gap. *J Sound Vib* 2022;540:117297.
- [28] Zhou J, Wang K, Xu D, Ouyang H, Fu Y. Vibration isolation in neonatal transport by using a quasi-zero-stiffness isolator. *J Vib Control* 2017;24(15):3278–91.
- [29] Wu L, Liu L, Wang Y, Zhai Z, Zhuang H, Krishnaraju D, et al. A machine learning-based method to design modular metamaterials. *Extreme Mech. Lett* 2020:100657.
- [30] Li B, Shuai C, Xu W, Yang Z. Review on low frequency control of quasi-zero stiffness. In: 2021 13th international conference on computer and automation engineering (ICCAE); 2021. p. 59–63.
- [31] Zheng Y, Shanguan W, Yin Z, Liu X. Design and modeling of a quasi-zero stiffness isolator for different loads. *Mech Syst Signal Process* 2023;188:110017.
- [32] Zhang Q, Guo D, Hu G. Tailored mechanical metamaterials with programmable quasi-zero-stiffness features for full-band vibration isolation. *Adv Funct Mater* 2021;31(33):2101428.
- [33] Lu Z, Brennan MJ, Yang T, Li X, Liu Z. An investigation of a two-stage nonlinear vibration isolation system. *J Sound Vib* 2013;332(6):1456–64.
- [34] Wu L, Wang Y, Zhai Z, Yang Y, Krishnaraju D, Lu J, et al. Mechanical metamaterials for full-band mechanical wave shielding. *Appl Mater Today* 2020;20:100671.
- [35] Xu D, Yu Q, Zhou J, Bishop SR. Theoretical and experimental analyses of a nonlinear magnetic vibration isolator with quasi-zero-stiffness characteristic. *J Sound Vib* 2013;332(14):3377–89.
- [36] Koza JR. Genetic programming: on the programming of computers by means of natural selection. MIT Press; 1992. p. 680.
- [37] Dykstra DMJ, Lenting C, Masurier A, Coulais C. Buckling metamaterials for extreme vibration damping. *Adv Mater* 2023;35(35):2301747.



**Xinyu Song** is a student from Xi'an Jiaotong University. His research focuses on the optimization and performance prediction of vibration isolation metamaterials using machine learning algorithms. His work has been presented at notable conferences, including the 8th National Additive Manufacturing Young Scientists Forum, the 3rd Metamaterials Conference, and the 13th ACCM in Japan.



**Lingling Wu** is an associate professor in Xi'an Jiaotong University. Her research area is artificial intelligence-assisted mechanical metamaterial design. She has published more than 30 academic papers, on top international journals including *Advanced Science*, *Materials Today*, *Advanced Functional Materials*, and so on, with over 2200 citations on Google Scholar. She serves as the youth editorial board member for *CJME: Additive Manufacturing Frontier*, and was selected for the 9th China Association for Science and Technology Youth Talent Program.



**Hanqing Jiang** is a Chair Professor of Mechanical Engineering at Westlake University in China. Before joining Westlake University in June 2021, he was a faculty member of Mechanical Engineering at Arizona State University from 2006 to 2021. He received his Ph.D. degree from Tsinghua University in 2001, majoring in Solid Mechanics. His current research interests include the origami and kirigami based mechanical metamaterials and robotics, mechanics of lithium-metal batteries, and unconventional electronics. He has published 5 book chapters and more than 150 peer-reviewed journal papers. He was elected to an ASME Fellow in 2016. He is a member of the executive committee of the Materials Division of ASME and is

the President of the Society of Engineering Science in 2022. Selected honors include an NSF CAREER Award (2009), ASME Worcester Reed Warner Medal (2021), etc.